Journal of Natural Gas Science and Engineering 34 (2016) 428–438

Contents lists available at ScienceDirect

Journal of Natural Gas Science and Engineering

journal homepage: www.elsevier.com/locate/jngse

Thermodynamic analysis and optimization of a waste heat recovery system for proton exchange membrane fuel cell using transcritical carbon dioxide cycle and cold energy of liquefied natural gas

Mohammad Hossein Ahmadi [a, *], Amin Mohammadi [a], Fathollah Pourfayaz [a, **], Mehdi Mehrpooya [a], Mokhtar Bidi [b, ***], Antonio Valero [c], Sergio Uson [c]

[a] Department of Renewable Energies, Faculty of New Sciences and Technologies, University of Tehran, Tehran, Iran
[b] Faculty of Mechanical & Energy Engineering, Shahid Beheshti University, A.C., Tehran, Iran
[c] CIRCE, Center of Research for Energy Resources and Consumption, Mariano Esquillor n. 15, 50018 Zaragoza, Spain

ARTICLE INFO

Article history:
Received 13 May 2016
Received in revised form
12 June 2016
Accepted 5 July 2016
Available online 8 July 2016

Keywords:
Proton exchange membrane fuel cell
Transcritical carbon dioxide cycle
Liquefied natural gas
Waste heat recovery
Energy analysis
Optimization

ABSTRACT

Hybrid systems are receiving more and more attention due to their higher efficiencies compared with standalone systems. Higher efficiencies mean lower consumption of fuels and as a result lower environmental problems. In this paper, a hybrid system consists of a transcritical carbon dioxide cycle and a liquefied natural gas cycle is proposed to recover the waste heat produced in a proton exchange membrane fuel cell. A complete sensitivity analysis is performed on the system considering five key parameters, namely operating temperature of fuel cell, CO_2 turbine inlet temperature, CO_2 turbine inlet pressure and pinch temperature of condenser and preheater. Also to achieve the highest possible energy efficiency, an optimization technique is applied on the system. The results showed that using the proposed system, generated power of the system increases by 39% compared with a standalone fuel cell. Also its efficiency reached to 72% after optimization, while it was equal to 39% before using the waste heat recovery system.

1. Introduction

During the last two centuries, population growth rate has increased rapidly and this has led to a huge increment in energy consumption. Currently, fossil fuels are the main source of energy. The fact that these types of fuel are exhaustible and their consumption results in environmental problems make researchers to search for cleaner sources of energy (Omer, 2008). Hydrogen can be considered as the key solution as it is one of the best fuels due to its zero emission products. It can be used in a fuel cell to produce electricity, heat and water. There are different kinds of fuel cells. Among them, proton exchange membrane (PEM) fuel cell is the most promising one due to its quick startup time and better durability (Wu et al., 2008).

Many researchers have studied performance of PEM fuel cells. Peighambardoust et al. (2010) performed a review on PEM fuel cell in different applications. They also provide some information on calculating properties of the membrane such as its ion exchange capacity, water uptake, gas permeability, etc. Bıyıkoglu (Bıyıkoğlu, 2005) reviewed different methods for modeling a proton exchange membrane fuel cell and described governing equations and assumptions of each model. Amphlett et al. (1995) proposed a parametric model to evaluate performance of a PEM fuel cell. Wang et al. (2005) developed a dynamic model for PEM fuel cell and considered the effect of double-layer charging and thermodynamic characteristic inside the cell. The proposed model can be used to estimate the cell's electrical response under both steady state and transient conditions. Saeed and Warkozek (2015) proposed a mathematical model to simulate a renewable PEM fuel cell system which uses a photovoltaic module to produce electricity and then the generated electricity is used in a PEM electrolyzer to produce hydrogen for operation of a PEM fuel cell. Heidary et al. (2016) investigated the effect of placing blockages in channel flow field on the cell performance using experimental analysis. They considered two types of blockages, including in-line and staggered.

* Corresponding author.
** Corresponding author.
*** Corresponding author.
E-mail addresses: mohammadhosein.ahmadi@gmail.com (M.H. Ahmadi), pourfayaz@ut.ac.ir (F. Pourfayaz), m_bidi@sbu.ac.ir (M. Bidi).

http://dx.doi.org/10.1016/j.jngse.2016.07.014
1875-5100/

Ghanbarian and Kermani (2016) compared performance of a fuel cell with three types of indented channel with a base case channel. They also performed a sensitivity analysis on the influences of dent heights and arrangements exchange current density, fluid viscous resistance and rib sizes.

PEM fuel cells have high energy efficiency in comparison with other energy systems (Li and Sabir, 2005). This is due to direct conversion of chemical energy of hydrogen into electricity in the cell, while in other energy systems a series of energy conversion should occur to produce electricity which reduces their efficiency. Although efficiency of PEM fuel cells is high, based on the first law of thermodynamics, a part of the input chemical energy converts into heat. This heat can be used for other purposes to increase total efficiency of the system. One way to use this heat is to utilize it in a combined heat and power (CHP) system. Ellamla et al. (2015) performed a review on using fuel cell, especially PEM fuel cell for CHP systems in residential sector. Kang et al. (2016) modeled a PEM fuel cell based CHP in ASPEN HYSYS and assessed the influence of different operating parameters on the system performance. Briguglio et al. (2011) used a CHP system to recover the waste heat of a 5 kW PEM fuel cell and improve its efficiency and calculated thermal and electrical performances of the system. There are also other ways to recover this waste heat. Yang and Zhang (2015) performed a parametric analysis on a hybrid system consists of a PEM fuel cell and an absorption refrigeration system. They used the heat produced in fuel cell as the input energy to the absorption refrigeration system for cooling purposes. By using the proposed system, total energy efficiency of the system increases by 6.8%. Long et al. (2015) coupled a thermally regenerative electrochemical cycle to a PEM fuel cell to recover its waste heat and produce more electricity. They also used an optimization algorithm to optimize the output power of the system. Hasani and Rahbar (2015) recovered the waste heat produced in PEM fuel cell using a thermoelectric system. They also developed an empirical equation to determine the heat recovery system voltage using outlet water temperature of the PEM fuel cell. Chen et al. (2014) combined a PEM fuel cell with an irreversible three heat-source heat pump, and a regenerator to recover the produced heat in fuel cell. They derived an expression to evaluate output power and efficiency of the hybrid system and compared it with the results of the single cell performance. Nguyen et al. (2016) performed exergy analysis on a waste heat recovery system of a PEM fuel cell. The waste heat recovery system uses the heat produced in the cell to preheat its inlet air. They also evaluated energy efficiency of the proposed system and compared it with a system in which an external heater is used to preheat the inlet air.

Low temperature heat recovery cycles such as ORC cycle, Kalina cycle and transcritical carbon dioxide cycle are also good candidates to be coupled with PEM fuel cells to recover its waste heat. Zhao et al. (2012) used an ORC cycle to recover waste heat produced in a PEM fuel cell. They performed a sensitivity analysis on the most important parameters of the system, including the fuel flow rate, PEM fuel cell operating pressure, turbine inlet pressure and turbine backpressure. Implementation of such system boosts the efficiency of the system by 5%. Transcritical carbon dioxide cycles also show a good performance especially in low temperatures. Critical temperature of carbon dioxide is very low; as a result it can be easily converted into supercritical condition in operating temperature of PEM fuel cells or any other low temperature heat sources. There are some papers published on evaluation of CO_2 cycle. Zhao et al. (2015) performed energy and exergy analyses on a hybrid system composed of compressed air storage system, transcritical carbon dioxide cycle and liquefied natural gas (LNG) cycle. They used the cold energy of LNG to reduce inlet air temperature of the compressor to reduce its power consumption. Adding the LNG cycle, not only increases the system power generated, but also converts LNG into compressed natural gas with the help of removed energy in the CO_2 condenser. Song et al. (2012) carried out energy analysis on a transcritical CO_2 cycle which uses flat plat collector as heat source and LNG cycle as heat sink. They analyzed the effect of turbine inlet pressure, the turbine inlet temperature and the condensation temperature on the generated power and efficiency of the system. Wang et al. (2014) performed the same analysis on a system similar to Song's, except in their analysis they used geothermal energy as their heat source. They also optimized the plants performance using multi objective optimization. Xia et al. (2014) analyzed a solar powered CO_2 cycle and used the generated power of this system to produce fresh water using a RO desalination system. They also performed a parametric analysis along with an optimization to improve system performance. They showed that the proposed system can provide 2537 m^3 fresh water per day with an exergy efficiency of 4.9%.

In this paper, a novel system based on transcritical carbon dioxide cycle and LNG cycle is used to recover the waste heat produced in a PEM fuel cell. Employing the proposed system can bring about the following benefits: (1) boosting energy efficiency of the total system (2) increasing total generated power of the system (3) producing some chilled water for refrigeration purposes (4) converting LNG into natural gas without any further energy usage. The effect of the most important parameters on the total system performance is assessed using a sensitivity analysis and optimum values of these parameters are found using optimization technique to maximize energy efficiency of the system.

2. System description

The proposed system for waste heat recovery of proton exchange membrane fuel cell is shown in Fig. 1. Air and fuel are fed to the cathode and anode of the fuel cell, respectively and participate in electrochemical reactions to produce power. Besides the generated electricity, a huge amount of heat is also produced in the cell as byproduct. The produced heat should be removed from the stack to prevent it from degradation. Usually water is employed to absorb this heat and then the heated water can be used for CHP applications. In the proposed system, water circulation is replaced by a transcritical carbon dioxide cycle which uses the produced heat in the fuel cell as heat source. Fig. 2 shows the T-s diagram of transcritical carbon dioxide cycle. Critical temperature and pressure of carbon dioxide equals to 30.97 °C and 73.77 bar. Due to this low critical temperature, carbon dioxide can be easily converted into supercritical condition absorbing the heat produced in the fuel cell. The produced supercritical carbon dioxide expands in the turbine and generates power. On the other hand, CO_2 turbine outlet temperature is very low (around −40°C at 6 bar). As a result, water cooled condenser cannot be employed. In order to condense turbine outlet stream, LNG is used in the condenser. Utilization of LNG helps to increase net output power of the system and also provide some chilled water that can be used for refrigeration purposes. In general, the proposed cycle allows us to remove the produced heat in the fuel cell and use it to generate more power. It also provides some chilled water and natural gas. The produced natural gas could be converted into hydrogen to provide the inlet fuel to the stack.

3. Mathematical modeling

3.1. Electrochemical model of PEM fuel cell

A zero-dimensional PEM fuel cell model is represented in this section. To do this, the following assumptions are made to simplify the model:

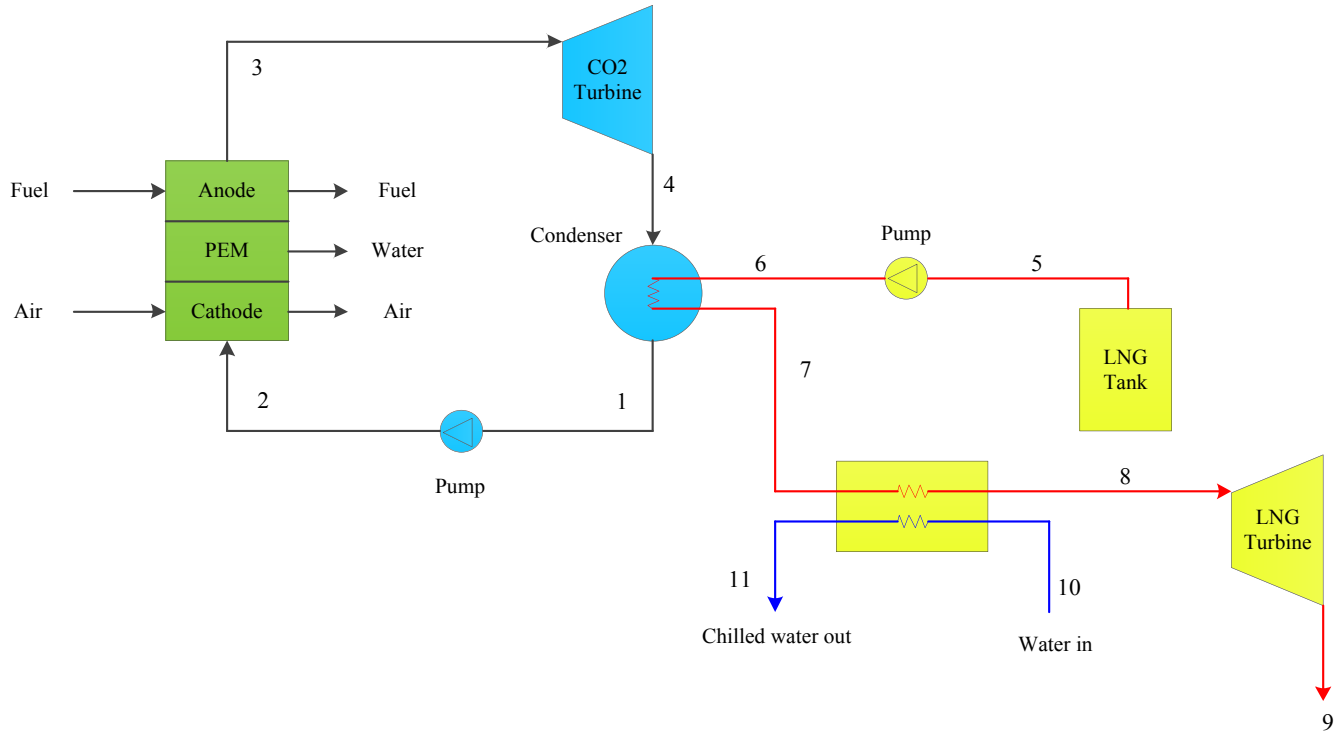

Fig. 1. Schematic diagram of the proposed cycle for waste heat recovery of PEM fuel cell.

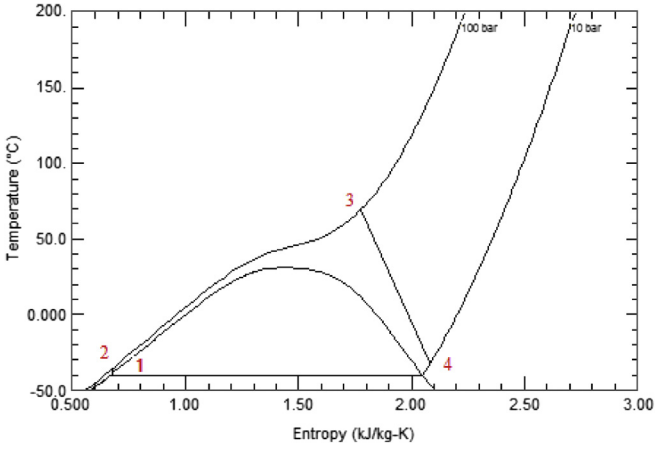

Fig. 2. T-s diagram of transcritical carbon dioxide cycle.

- The system is in steady state conditions.
- Chemical reactions reach to equilibrium state.
- Operating temperature and pressure of fuel cell equal to 85 °C and 3 bar.
- It is assumed that temperature is distributed uniformly across the fuel cell stack and temperature of the outlet product of the fuel cell is equal to the operating temperature of the cell.
- Pressure drop inside the fuel cell is neglected and outlet products pressure equals to the operating pressure of the cell.
- Fuel cell stack is fully insulated and heat transfer to the ambient is equal to zero.
- It is assumed that inlet air consists of 79% N_2 and 21% O_2.

As explained in the previous section, air and hydrogen are the reactants of the fuel cell. At anode, hydrogen losses electron and converts into hydrogen ion. The released electron goes through external circuit, while hydrogen ion passes the electrolyte. At the cathode, electron, ion hydrogen and oxygen react and produce water and heat. These reactions can be shown as follows:

$$Anode : H_2 \rightarrow 2H^+ + 2e^-$$

$$Cathode : 2H^+ + 2e^- + 0.5O_2 \rightarrow H_2O + Heat$$

Overall reaction of the cell is the combination of these two reactions:

$$H_2 + 0.5O_2 \rightarrow H_2O$$

The reversible open circuit voltage of a fuel cell can be calculated using Equation (1) (Mann et al., 2000):

$$E_{nernst} = 1.229 - 0.8 \times 10^{-3}\left(T_{fc} - 298.15\right) + 4.3085 \times 10^{-5} T_{fc} ln\left(P_{H_2} P_{O_2}^{0.5}\right) \quad (1)$$

In Equation (1), T_{fc} is the operating temperature of fuel cell in Kelvin and P_{H_2} and P_{O_2} are the partial pressures of hydrogen and oxygen in anode and cathode, respectively. To calculate the partial pressures, $P_{H_2O}^{sat}$ which is the saturation pressure of water vapor should be calculated first (Miansari et al., 2009):

$$\log\left(P_{H_2O}^{sat}\right) = -2.1794 + 0.02953\left(T_{fc} - 273.15\right) - 9.1837 \times 10^{-5}\left(T_{fc} - 273.15\right)^2 + 1.4454 \times 10^{-7}\left(T_{fc} - 273.15\right)^3 \quad (2)$$

Then the effective partial pressure of hydrogen and oxygen are computed by (Amphlett et al., 1995):

$$P_{H_2} = 0.5P_{H_2O}^{sat}\left(\frac{1}{\exp\left(1.653i/T_{fc}^{1.334}\right)x_{H_2O}^{sat}} - 1\right) \quad (3)$$

$$P_{O_2} = P\left(1 - x_{H_2O}^{sat} - x_{N_2}^{channel}\exp\left(0.291i/T_{fc}^{0.832}\right)\right) \quad (4)$$

In these equations, i is the current density and P is operating pressure of the cell. Also $x_{H_2O}^{sat}$ is the molar fraction of water which can be determined by:

$$x_{H_2O}^{sat} = \frac{P_{H_2O}^{sat}}{P} \quad (5)$$

Also $x_{N_2}^{channel}$ is the molar fraction of nitrogen in the air stream and calculated using Equations (6)–(8).

$$x_{N_2}^{channel} = \frac{\left(x_{N_2,in} - x_{N_2,out}\right)}{ln\left(x_{N_2,in}/x_{N_2,out}\right)} \quad (6)$$

$$x_{N_2,in} = 0.79\left(1 - x_{H_2O}^{sat}\right) \quad (7)$$

$$x_{N_2,out} = \frac{1 - x_{H_2O}^{sat}}{1 + \left(\frac{0.21}{0.79}\right)\left(\frac{\lambda_{air}-1}{\lambda_{air}}\right)} \quad (8)$$

Where λ_{air} is the stoichiometric rate of air. By using the above formula, open circuit voltage of the cell can be computed. Because of irreversible losses in the cell, actual obtained voltage of the cell is lower than the open circuit voltage. These irreversibilities can be divided into three categories, namely activation losses, ohmic losses and concentration losses. Actual voltage of a cell equals to the Nernst voltage minus these losses as (Murugesan and Senniappan, 2013):

$$V_{fc} = E_{nernst} - V_{act} - V_{ohm} - V_{conc} \quad (9)$$

The activation loss is a function of temperature, partial pressures of oxygen and hydrogen and the catalyst used in the electrodes. The following semi-empirical equation is used to calculate activation loss (Chen, 2011):

$$V_{act} = -\left[\xi_1 + \xi_2 T_{fc} + \xi_3 T_{fc} ln\left(C_{O_2}\right) + \xi_4 T_{fc} ln(I)\right] \quad (10)$$

where ξ_i are parametric coefficients defined as follows:

$$\xi_1 = -0.948 \quad (11)$$

$$\xi_2 = 0.00286 + 0.0002\ln\left(A_{fc}\right) + 4.38 \times 10^{-5}\ln\left(C_{H_2}\right) \quad (12)$$

$$\xi_3 = 7.6 \times 10^{-5} \quad (13)$$

$$\xi_1 = -1.93 \times 10^{-4} \quad (14)$$

Also I is the current of the cell which is expressed as:

$$I = iA_{fc} \quad (15)$$

Finally C_{O_2} and C_{H_2} are oxygen and hydrogen concentration on the catalytic interface (Chen, 2011):

$$C_{O_2} = 1.97 \times 10^{-7} P_{O_2}\exp\left(\frac{498}{T_{fc}}\right) \quad (16)$$

$$C_{H_2} = 9.174 \times 10^{-7} P_{H_2}\exp\left(\frac{-77}{T_{fc}}\right) \quad (17)$$

Ohmic loss occurs because of electrical resistance in fuel cell components. This resistance exists in membrane, in connections between the electrodes and in connections between the interface and the external circuit and the membrane. The value of this loss is calculated using the Ohmic's law (Corrêa et al., 2004):

$$V_{ohm} = I(R_m + R_c) \quad (18)$$

In Equation (18), R_c is the constant part of cell's resistance and R_m is a function of temperature and current density. Its value is computed using Equation (19):

$$R_m = \frac{r_{mem}L}{A_{cell}} \quad (19)$$

where L is the membrane thickness and r_{mem} is the specific membrane resistance and is expressed as:

$$r_{mem} = \frac{181.6\left(1 + 0.03i + 0.062\left(T_{fc}/303\right)^2 i^{2.5}\right)}{(\Psi - 0.634 - 3i)\exp\left(4.18\left(T_{fc} - 303\right)/T_{fc}\right)} \quad (20)$$

It should be noted that Ψ is an indicator of membrane hydration. If the membrane is fully hydrated, Ψ equals 14 and if membrane is fully saturated it equals to 23.

Concentration loss happens due to mass transfer limits. Increasing reactants rate results in a situation in which a huge amount of the reactants leaves the cell without being utilized. Therefore, overall voltage of the cell decreases. This phenomenon is known as concentration loss and can be determined by (Wang et al., 2005):

$$V_{conc} = \frac{RT_{fc}}{n_e F} ln\left(\frac{i_L}{i_L - i}\right) \quad (21)$$

where R is the universal gas constant, n_e is the number of electrons, F is Faraday constant and i_L is the maximum current density.

By using Equations 9–21, actual obtained voltage of the cell can be calculated. Fuel cell stack is comprised of many single cells connected together. Total power generated by the stack is obtained by:

$$W_{fc} = N_{cell} I V_{fc} \quad (22)$$

where N_{cell} represents total number of single fuel cells in the stack.

3.2. Thermal model of PEM fuel cell

As mentioned earlier, a fuel cell consumes air and hydrogen and produces electricity, water and heat. To calculate thermal model of the cell, molar flow rate of reactants and products should be computed. These values depend on total number of cells in the stack and the overall current as follows (Wang et al., 2005):

$$\dot{n}_{H_2,cons} = \frac{N_{cell} I}{2F} \quad (23)$$

$$\dot{n}_{O_2,cons} = \frac{N_{cell} I}{4F} \tag{24}$$

$$\dot{n}_{H_2O,gene} = \frac{N_{cell} I}{2F} \tag{25}$$

Since a part of reactants leaves the cell without any reaction, molar flow rate of reactants should be higher than their consumption (Van Nguyen and Knobbe, 2003). Actual values of reactants inlet molar flow can be determined by:

$$\dot{n}_{H_2,inlet} = \lambda_{H_2} \dot{n}_{H_2,cons} \tag{26}$$

$$\dot{n}_{O_2,inlet} = \lambda_{O_2} \dot{n}_{O_2,cons} \tag{27}$$

In these equations, λ_{H_2} and λ_{O_2} are the stoichiometric rate of hydrogen and oxygen.

Having the molar flow rates of reactants and products, energy balance of the fuel cell can be expressed as:

$$\dot{Q}_{net} = \dot{Q}_{ch} - \dot{W}_{fc} - \dot{Q}_{sl} \tag{28}$$

In Equation (28), $\dot{Q}_{ch}$ is the energy that is provided by electrochemical reactions. Its value is determined by:

$$\dot{Q}_{ch} = \dot{n}_{H_2,cons}\, HHV \tag{29}$$

Also $\dot{Q}_{sl}$ is the latent and sensible heat and can be estimated by (Wang et al., 2005):

$$\dot{Q}_{sl} = C_{p,H_2}\left(\dot{n}_{H_2,out}T_{fc} - \dot{n}_{H_2,in}T_{in}\right) + C_{p,O_2}\left(\dot{n}_{O_2,out}T_{fc} - \dot{n}_{O_2,in}T_{in}\right) + C_{p,N_2}\left(\dot{n}_{N_2,out}T_{fc} - \dot{n}_{N_2,in}T_{amb}\right) + C_{p,H_2O}\dot{n}_{H_2O,gene}\left(T_{fc} - T_{amb}\right) + \dot{n}_{H_2O,gene}H_v \tag{30}$$

Where C_{p,H_2}, C_{p,O_2}, C_{p,N_2} and C_{p,H_2O} are the specific heat capacity of hydrogen, oxygen, nitrogen and water respectively and H_v is the vaporization heat of water. Table 1 represents value of constant parameters used in PEM modeling.

3.3. Transcritical carbon dioxide cycle

A steady state transcritical carbon dioxide cycle is illustrated in this section. The following assumptions are made to simplify the model:

- The system operates under steady state conditions.
- A constant pressure drop is considered for all components, except condenser.
- A constant isentropic efficiency is assumed for pumps and turbines.
- All components are considered to be adiabatic.
- Condenser outlet stream is assumed to be saturated liquid.

As mentioned above, carbon dioxide should absorb produced heat in the fuel cell stack which is equal to Q̇net obtained by Equation (28). Energy balance for PEM fuel cell as control volume is expressed as:

$$\dot{Q}_{net} = \dot{m}(h_3 - h_2) \tag{31}$$

Power generated by CO_2 turbine can be determined as:

$$\dot{W}_{tur} = \dot{m}(h_{in} - h_{out}) \tag{32}$$

Enthalpy of turbine outlet stream can be calculated using its isentropic efficiency:

$$\eta_{tur} = \frac{h_{in} - h_{out}}{h_{in} - h_{out,s}} \tag{33}$$

In condenser, turbine outlet stream should convert into saturated liquid. The heat rejected by this process is used to increase temperature of LNG and convert it into natural gas. Energy balance for the condenser is defined as follows:

$$\dot{m}_1\,(h_4 - h_1) = \dot{m}_6\,(h_7 - h_6) \tag{34}$$

Also the following temperature equation exists between LNG and CO_2 streams:

$$T_7 = T_4 - pinch_{condenser} \tag{35}$$

Consumed power by pump can be computed using Equations (36) And (37).

$$\dot{W}_{pump} = \dot{m}(h_{out} - h_{in}) \tag{36}$$

$$\eta_{pump} = \frac{h_{in} - h_{out,s}}{h_{in} - h_{out}} \tag{37}$$

In preheater, using the surplus cold energy in LNG, some chilled water can be produced. Mass flow rate of chilled water can be determined by:

$$\dot{m}_7\,(h_7 - h_8) = \dot{m}_{10}\,(h_{10} - h_{11}) \tag{38}$$

Also the following relation exists between temperature of water and LNG:

$$T_8 = T_{10} - pinch_{preheater} \tag{39}$$

Table 2 lists the assumed constant parameters used to model the transcritical CO2 cycle.

3.4. Total system performance

Total system performance can be evaluated by net generated power and efficiency of PEM fuel cell and CO_2 and LNG cycles. Net generated power of the hybrid system is determined by:

Table 1
Constant parameters used in PEM modeling.

Parameter	Unit	Value
Ambient temperature (T_{amb})	K	298
Ambient temperature (P_{amb})	bar	1.01
Operating temperature (T_{fc})	K	358.15
Operating pressure (P_{fc})	bar	3
Number of electrons (n_e)	–	2
Faraday constant (F)	C/mol	96,485
Universal gas constant (R)	J/mol K	8.314
Number of cells (N_{cell})	–	13,000
Active surface area (A_{cell})	cm^2	232
Current density (i)	A/cm^2	0.6
Maximum current density (i_L)	A/cm^2	1.5
Membrane thickness (L)	cm	0.0178
Stoichiometric rate of hydrogen (λ_{H_2})	–	1.2
Stoichiometric rate of oxygen (λ_{O_2})	–	2
Higher heating value (HHV)	kJ/mol	285.55

Table 2
Constant parameters of transcritical carbon dioxide and LNG cycle.

Parameter	Unit	Value
CO_2 turbine inlet temperature	C	70
CO_2 turbine inlet pressure	bar	100
Condenser pressure	bar	6
Outlet temperature of chilled water	C	5
Isentropic efficiency of turbine	%	85
Isentropic efficiency of pump	%	75
LNG temperature	C	−161.7
LNG pressure	bar	1.01
Condenser pinch temperature	C	50
Preheater pinch temperature	C	15
Pressure drop in vapor generator	%	3
Pressure drop in preheater	%	1

$$\dot{W}_{net} = \dot{W}_{fc} + \sum \dot{W}_{tur} - \sum \dot{W}_{pump} \tag{40}$$

Thermal efficiency of the PEM fuel cell is calculated using the following equation:

$$\eta_{fc} = \frac{\dot{W}_{fc}}{\dot{n}_{H_2,cons}\, HHV} \tag{41}$$

Finally, net energy efficiency of the system is expressed as:

$$\eta_{net} = \frac{\dot{W}_{net} + \dot{m}_{10}\,(h_{10} - h_{11})}{\dot{n}_{H_2,cons}\, HHV_{H_2} + \dot{m}_5\,(h_9 - h_5)} \tag{42}$$

4. Optimization

There are many techniques that could be used to optimize the plants performance, including genetic algorithm, particle swarm optimization, ant colony optimization, etc. Among them, genetic algorithm is a well-known method which has the ability to deal with linear and nonlinear constrains. It was developed by Holland (Holland, 1975) and is based on Darwin's theory which states that the fittest ones have higher chances to survive. To perform the optimization, GA first produces some random numbers which are called the chromosomes. Each of these chromosomes is evaluated and their fitness value is computed. The best chromosomes are transferred to the next generation. In this step, GA uses mating procedure (crossover and mutation operators) to generate new chromosomes for the next generation. This process continues until the algorithm converges and the optimum solution is found. Fig. 3 shows the flowchart of optimization algorithm. More explanation about genetic algorithm is provided in (Coley, 1999; Sivanandam and Deepa, 2007).

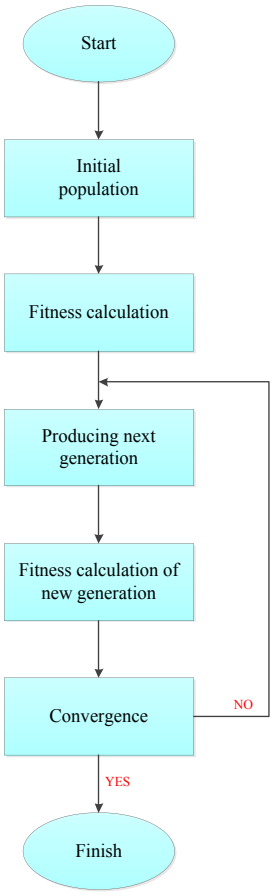

Fig. 3. Flowchart of optimization algorithm (Vandani et al., 2015).

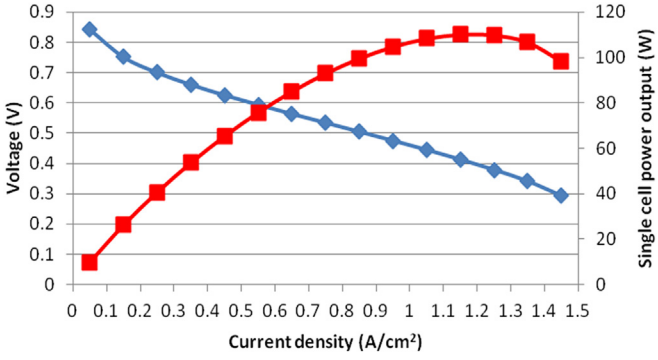

Fig. 4. Polarization curve of the PEM fuel cell.

5. Results and discussion

To evaluate performance of the proposed system, a simulation program is developed in Matlab using equations provided in section 3. Thermodynamic properties of carbon dioxide and LNG are calculated using REFPROP (Lemmon et al., 2007). Proton exchange membrane fuel cell is the heart of the system which generates power and provides heat for waste heat recovery system. Fig. 4 represents variation of cell voltage and its output power versus current density. As can be seen, with increasing current density, overall voltage decreases. The reason behind that is with increasing current density, voltage losses increases in the cell and this reduces overall voltage. Activation loss has the key role in this reduction, while the values of two other losses are far lower than the activation loss. On the other hand, variation of fuel cell output power is completely different with cell voltage and it has a maximum at 1.15 A/cm^2.

Table 3 gives information about thermodynamic properties of each stream in the cycle and Table 4 shows performance indicators of the fuel cell and waste heat recovery system.

It can be observed that under situation provided in Table 1, fuel cell stack consumes 11.25 mol per second hydrogen. After electrochemical reactions, 1047.58 kW electricity is generated by stack. Also a total amount of 1189.38 kW heat is produced which should be transferred to the working fluid in transcritical CO_2 cycle. This heat is recovered by waste heat recovery system and converts into

Table 3
Thermodynamic properties of each stream in the waste heat recovery cycle.

Stream	Working fluid	P [bar]	T [C]	h [kJ/kg]	s [kJ/kg K]	$\dot{m}$ [kg/s]
1	CO_2	6	−53.12	86.796	0.552	3.372
2	CO_2	103.09	−48.76	97.899	0.565	3.372
3	CO_2	100	70	450.653	1.780	3.372
4	CO_2	6	−53.12	371.124	1.844	3.372
5	LNG	1.01	−161.70	−0.756	−0.007	4.693
6	LNG	70	−158.33	21.007	0.042	4.693
7	LNG	66.50	−103.12	225.296	1.491	4.693
8	LNG	65.84	10	803.222	4.206	4.693
9	LNG	40	−21.50	752.735	4.242	4.693
10	Water	1.01	25	104.920	0.367	32.363
11	Water	1.01	5	21.120	0.076	32.363

Table 4
Generated power and energy efficiency of each component and total cycle.

Parameter	Unit	Value
$\dot{n}_{H_2,inlet}$	Mole/s	11.25
$\dot{W}_{fc}$	kW	1047.58
$\dot{Q}_{net}$	kW	1189.38
η_{fc}	%	39.12
$\dot{W}_{CO_2,tur}$	kW	268.15
$\dot{W}_{CO_2,pump}$	kW	37.43
$\dot{W}_{LNG,tur}$	kW	236.92
$\dot{W}_{LNG,pump}$	kW	102.13
$\dot{W}_{net}$	kW	1413.08
η_{net}	%	66.39

electricity in CO_2 and LNG turbines. Adding this waste heat recovery cycle improves total generated power of the cycle by 34%. It also enhances total system efficiency considerably. Before implementation of the proposed system, total efficiency was equal to 39.12% which was efficiency of the fuel cell, while after introducing this new system, it increases to 66.39%.

5.1. Sensitivity analysis

To evaluate the effect of different parameters on the system performance, a complete sensitivity analysis is performed on the cycle. Five parameters are considered to perform the analysis, including operating temperature of fuel cell, CO_2 turbine inlet temperature, CO_2 turbine inlet pressure, pinch temperature of condenser and pinch temperature of preheater. The effects of each of these parameters on the system performance are studied in the following.

5.1.1. Effect of operating temperature of fuel cell

Fig. 5 shows the effect of fuel cell operating temperature on generated power. Generated power by fuel cell is calculated by multiplying cell voltage by its current. Current is a function of current density and fuel cell active area which both of them are assumed to be constant. As a result, fuel cell current remains unchanged. Therefore, variation of fuel cell power is directly related to variation of its voltage. Increasing operating temperature of fuel cell decreases voltage loss in the cell which leads to an increment in fuel cell generated power. As shown in Equation (23), molar flow rate of inlet hydrogen is dependent on the current of the cell. Since current is constant, molar flow rate of hydrogen remains constants too. Consequently, total energy input to the cell ($\dot{Q}_{ch}$) is constant. Based on Equation (28) with increasing $\dot{W}_{fc}$, $\dot{Q}_{net}$ decreases. This means that lower amount of energy delivers to the waste heat recovery

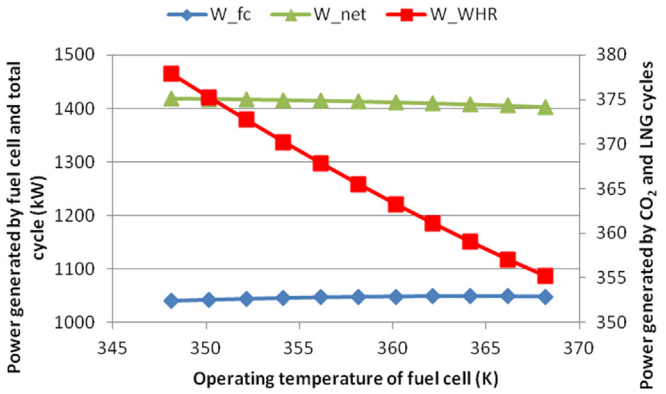

Fig. 5. Effect of operating temperature of fuel cell on generated power.

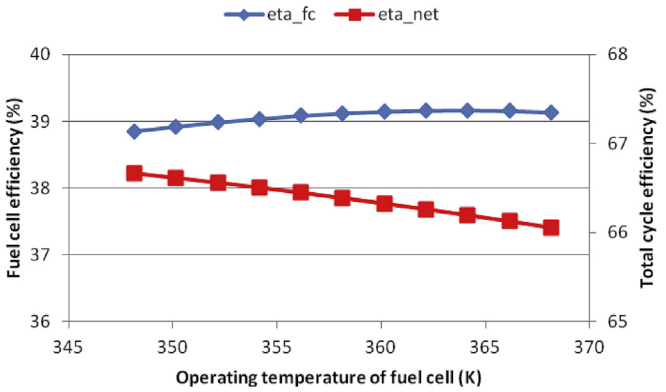

Fig. 6. Effect of operating temperature of fuel cell on energy efficiency of fuel cell and total cycle.

system and as a result, generated power by CO_2 and LNG turbine decreases. In general, since reduction of generated power by CO_2 and LNG turbine is higher than increment in generated power by fuel cell, net output power of the system decreases slightly.

Since molar flow rate of hydrogen is constant and fuel cell generated power is increasing, based on Equation (41), energy efficiency of fuel cell increases. On the other hand, since total output power decreases, total efficiency of the plant decreases too (see Fig. 6).

5.1.2. Effect of CO_2 turbine inlet temperature

Fig. 7 shows variation of generated power by changing CO_2

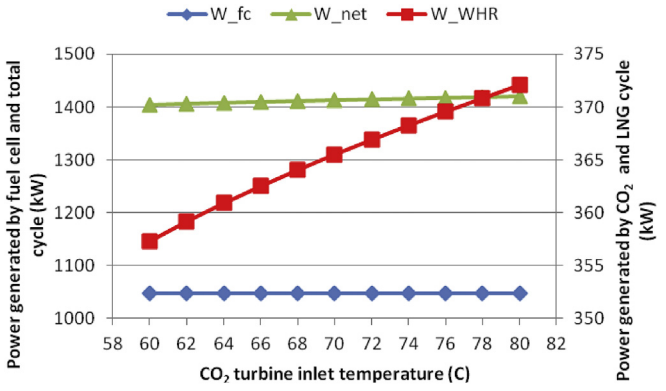

Fig. 7. Effect of CO_2 turbine inlet temperature on generated power.

turbine inlet temperature. Since CO_2 cycle is placed downstream of the fuel cell, any changes in its operating parameters do not affect performance of the fuel cell. As a result, generated power by fuel cell remains constant. On the other hand, since Q_{net} is constant, when turbine inlet temperature raises it increases enthalpy of turbine inlet stream and reduces mass flow rate of produced CO_2 simultaneously. In general it leads to an increment in generated power by CO_2 turbine. On the other hand, since mass flow rate of carbon dioxide decreases, it results in reduction of produced LNG and consequently power generated by LNG turbine reduces slightly. In general, power generated by waste heat recovery system increases by increasing CO_2 turbine inlet temperature and therefore total generated power of cycle increases.

As mentioned above, variation of turbine inlet temperature does not change performance of the fuel cell as shown in Fig. 8. Therefore, energy efficiency of fuel cell does not vary. Also total cycle efficiency increases due to increasing net generated power.

5.1.3. Effect of CO_2 turbine inlet pressure

Figs. 9 and 10 show the effect of CO_2 turbine inlet pressure on generated power and efficiency of the system. Similar to the previous case, it does not change generated power by fuel cell. On the other hand, generated power by CO_2 turbine increases at first with increasing turbine inlet pressure and reach to a maximum. After that it decreases. It means that for each turbine inlet temperature, there is an optimum value for turbine inlet pressure which results in maximum generated power. Also net output power of the system has a maximum which is equal to 1413 kW at 95 bar.

Since molar flow rate of hydrogen remains constant, efficiency of the system is only a function of its generated power. Since net output power of the system has a maximum with variation of turbine inlet pressure, total energy efficiency of the system has a maximum too.

5.1.4. Effect of pinch temperature of CO_2 condenser

Fig. 11 shows the effect of pinch temperature of CO_2 condenser on generated power. As can be seen, its effect is considerable on generated power by waste heat recovery system. Variation of pinch temperature can only affect LNG cycle. When it increases, mass flow rate of LNG in the cycle raises which results in higher power production by LNG turbine. Another effect of this variation is that when pinch temperature increases, temperature of condenser outlet stream (stream 7) decreases. As a result, more cold energy is available in preheater and consequently more chilled water can be produced. Based on Equation (42), the aforementioned variations lead to an increment in total energy efficiency of the system (Fig. 12). It is worth mentioning that between all considered parameters, pinch temperature of CO_2 condenser is the most effective parameter.

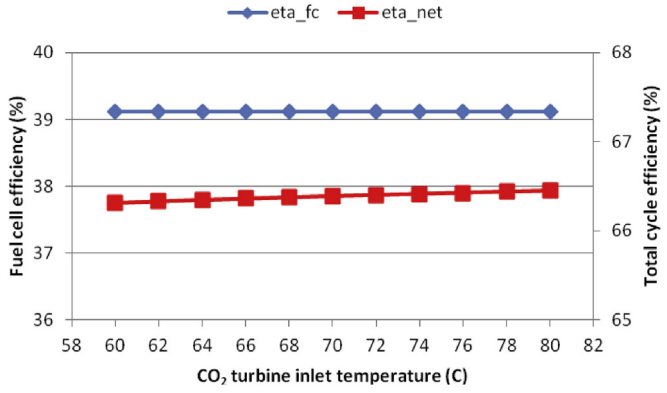

Fig. 8. Effect of CO_2 turbine inlet temperature on energy efficiency of fuel cell and total cycle.

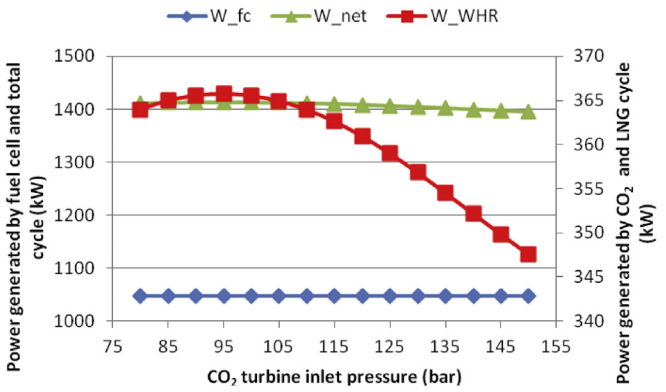

Fig. 9. Effect of CO_2 turbine inlet pressure on generated power.

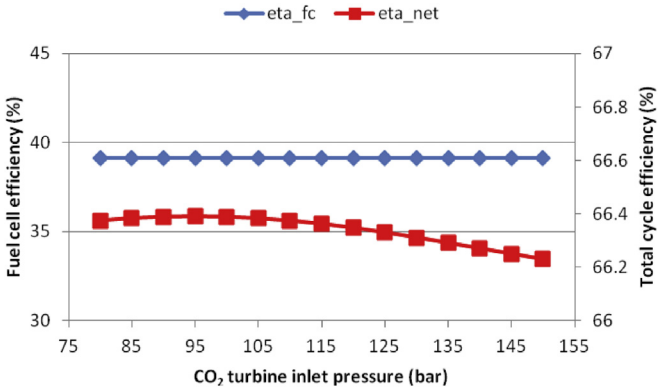

Fig. 10. Effect of CO_2 turbine inlet pressure on energy efficiency of fuel cell and total cycle.

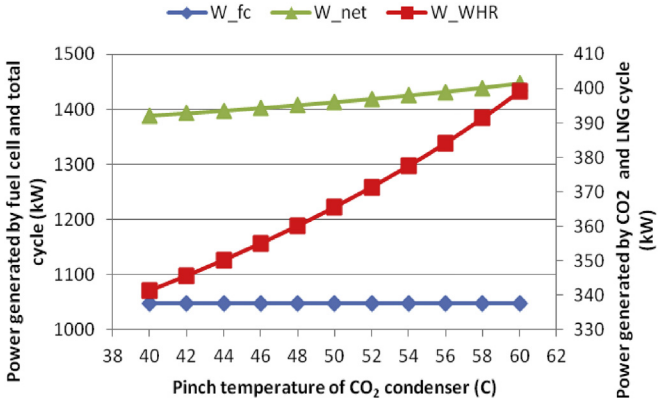

Fig. 11. Effect of pinch temperature of CO_2 condenser on generated power.

5.1.5. Effect of pinch temperature of preheater

Figs. 13 and 14 show the effect of pinch temperature of preheater. Variation of this parameter can only affect power generated by LNG turbine and mass flow rate of produced chilled water. Unlike the previous case in which increasing pinch temperature leads to an increment in generated power and efficiency, in this case,

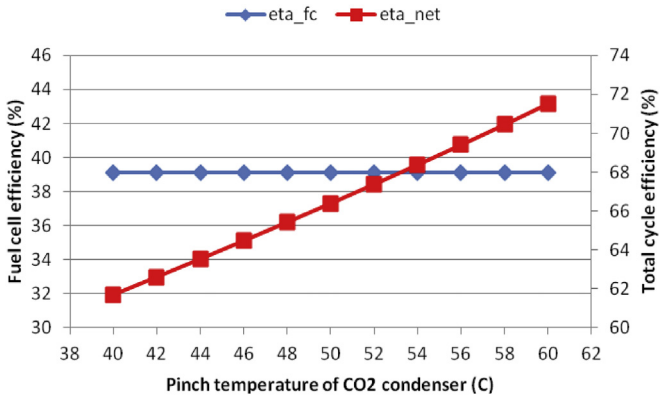

Fig. 12. Effect of pinch temperature of CO_2 condenser on energy efficiency of fuel cell and total cycle.

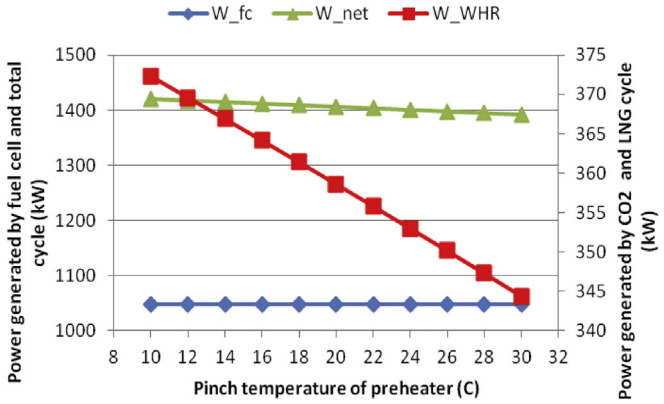

Fig. 13. Effect of pinch temperature of preheater on generated power.

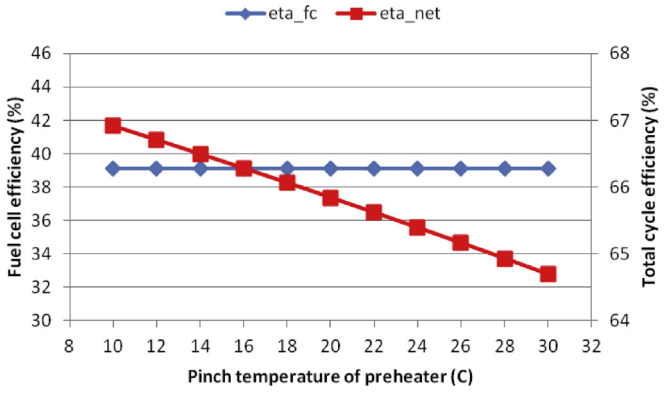

Fig. 14. Effect of pinch temperature of preheater on energy efficiency of fuel cell and total cycle.

performance of the plant deteriorates. This could be explained by noting that based on Equation (39), when pinch temperature increases, temperature of stream 8 decreases. As a result, LNG turbine inlet enthalpy decreases which itself reduces generated power by LNG turbine. Therefore, net generated power of system decreases.

Also the higher the pinch temperature, the lower the produced mass flow rate of chilled water. Simultaneous reduction of net output power and produced mass flow rate of chilled water lead to reduction in energy efficiency of the system as shown in Fig. 14.

5.2. Optimization results

To find out the optimum value of each parameter an optimization technique is performed using genetic algorithm to maximize energy efficiency of the system. Five decision variables are considered in this section, namely, operating temperature of PEM fuel cell, CO_2 turbine inlet temperature, CO_2 turbine inlet pressure, pinch temperature of condenser and pinch temperature of preheater.

Table 5 lists the decision variables along with their lower and upper boundaries. It should be noted that turbine inlet temperature is directly dependent on operating temperature of fuel cell. As a result, it cannot be selected as a decision variable. Therefore, the following relation is defined between operating temperature of fuel cell and CO_2 turbine inlet temperature.

$$T_3 = T_{fc} - pinch_{PEM} \tag{43}$$

$pinch_{PEM}$ is the dependent parameter that is used in the optimization process.

Optimum value of each decision variable and the corresponding optimum efficiency of the system are shown in Table 6.

Table 7 compares performance of the system before and after optimization. As can be seen, total energy efficiency of the system which was the objective function of optimization process, increased to 72.36% which shows 9% increment in its efficiency compared with before optimization. Changes in other performance indicators are also shown in the table. In optimum conditions, since operating temperature of fuel cell decreases, generated power by fuel reduces too. On the other hand, with optimum values of CO_2 turbine inlet temperature and pressure, generated power CO_2 cycle increases by 2.9%. Also optimum values of pinch temperature in condenser and preheater lead to an increment in mass flow rate of produced natural gas and chilled water. With increasing mass flow rate of natural gas, produced power in LNG turbine increases by 32% which is very considerable.

6. Conclusion

A hybrid system consists of a transcritical carbon dioxide cycle and a LNG cycle is proposed to recover waste heat produced in a PEM fuel cell. To investigate the effect of different parameters, a complete sensitivity analysis is performed on the cycle. Also an optimization technique is employed to find the optimum values of

Table 5
Lower and upper boundary of each decision variable.

Decision variable	Unit	Lower boundary	Upper boundary
Operating temperature of fuel cell	K	348.15	368.15
Pinch temperature of PEM fuel cell	C	5	15
CO_2 turbine inlet pressure	bar	80	150
Pinch temperature of condenser	C	40	60
Pinch temperature of preheater	C	10	30

Table 6
Optimum value of decision variables and corresponding optimum efficiency.

Parameter	Unit	Optimum value
Operating temperature of fuel cell	K	348.15
Pinch temperature of PEM fuel cell	C	5
CO_2 turbine inlet pressure	bar	97.71
Pinch temperature of condenser	C	60
Pinch temperature of preheater	C	10
Total system efficiency	%	72.36

Table 7
Performance of the system in optimum condition.

Parameter	Unit	Before optimization	After optimization
Generated power by fuel cell	kW	1047.6	1040.5
Generated power by CO_2 turbine	kW	268.15	276.04
Consumed power by CO_2 pump	kW	37.43	37.36
Generated power by LNG turbine	kW	236.92	314.76
Consumed power by LNG pump	kW	102.13	131.90
Mass flow rate of produced natural gas	kg/s	4.69	6.06
Mass flow rate of produced chilled water	kg/s	32.36	45.75
Efficiency of fuel cell	%	39.12	38.86
Efficiency of total system	%	66.39	72.36

the considered decision variables to maximize energy efficiency of the system. The main conclusions of the study are summarized as follows:

- The new system has the ability to convert waste heat into electricity and therefore increase net output power of the system. It can also provide some chilled water and convert LNG into natural gas. These changes lead to an increment in energy efficiency of the hybrid system.
- Sensitivity analysis showed that increasing operating temperature of fuel cell and pinch temperature of preheater reduce plants efficiency, while increasing CO_2 turbine inlet temperature and pinch temperature of condenser increase it. Also there is an optimum value for CO_2 turbine inlet pressure which leads to maximum efficiency.
- Optimization results showed that in optimum conditions, total generated power of system can increase by 39.56% compared with a standalone fuel cell. Also efficiency of the system increases by 9% compared to situation before optimization.

Nomenclature

A_{fc}	Active surface area of fuel cell (cm^2)
C	Concentration (mol/cm^3)
C_p	Specific heat capacity (J/molK)
E_{nernst}	Open circuit voltage (V)
F	Faraday constant (C/mol)
h	Enthalpy (kJ/kg)
HHV	Higher heating value (kJ/mol)
I	Current (A)
i	Current density (A/cm^2)
i_L	Maximum current density (A/cm^2)
L	Membrane thickness (cm)
$\dot{m}$	Mass flow rate (kg/s)
$\dot{n}$	Molar flow rate (mol/s)
N_{cell}	Number of cells in fuel cell stack
n_e	Number of electrons
P	Pressure (bar)
$P^{sat}_{H_2O}$	Saturation pressure of water vapor (bar)
$\dot{Q}$	Heat (kW)
R	Universal gas constant (J/molK)
r_{mem}	Membrane resistivity (ohm cm)
s	Entropy (kJ/kgK)
T	Temperature (K),(C)
V	Voltage (V)
$\dot{W}$	Power (kW)
WHR	Waste heat recovery
x	Molar fraction

Greek letters

η	Isentropic efficiency
λ	Stoichiometric rate
Ψ	Membrane hydration

Subscripts

act	Concentration
conc	Activation
cons	Consumption
fc	Fuel cell
gene	Generation
H_2	Hydrogen
H_2O	Water
N_2	Nitrogen
O_2	Oxygen
ohm	Ohmic
tur	turbine

References

Amphlett, J.C., Baumert, R., Mann, R.F., Peppley, B.A., Roberge, P.R., Harris, T.J., 1995. Performance modeling of the Ballard Mark IV solid polymer electrolyte fuel cell I. Mechanistic model development. J. Electrochem. Soc. 142, 1–8.

Briguglio, N., Ferraro, M., Brunaccini, G., Antonucci, V., 2011. Evaluation of a low temperature fuel cell system for residential CHP. Int. J. Hydrogen Energy 36, 8023–8029.

Bıyıkoğlu, A., 9//2005. Review of proton exchange membrane fuel cell models. Int. J. Hydrogen Energy 30, 1181–1212.

Chen, P.-C., 2011. The dynamics analysis and controller design for the PEM fuel cell under gas flowrate constraints. Int. J. Hydrogen Energy 36, 3110–3122.

Chen, X., Wang, Y., Zhou, Y., 2014. Equivalent power output and parametric optimum design of a PEM fuel cell-based hybrid system. Int. J. Electr. Power & Energy Syst. 63, 429–433.

Coley, D.A., 1999. An Introduction to Genetic Algorithms for Scientists and Engineers. World scientific.

Corrèa, J.M., Farret, F.A., Canha, L.N., Simões, M.G., 2004. An electrochemical-based fuel-cell model suitable for electrical engineering automation approach. Ind. Electron. IEEE Trans. 51, 1103–1112.

Ellamla, H.R., Staffell, I., Bujlo, P., Pollet, B.G., Pasupathi, S., 2015. Current status of fuel cell based combined heat and power systems for residential sector. J. Power Sources 293, 312–328.

Ghanbarian, A., Kermani, M., 2016. Enhancement of PEM fuel cell performance by flow channel indentation. Energy Convers. Manag. 110, 356–366.

Hasani, M., Rahbar, N., 2015. Application of thermoelectric cooler as a power generator in waste heat recovery from a PEM fuel cell–An experimental study. Int. J. Hydrogen Energy 40, 15040–15051.

Heidary, H., Kermani, M.J., Advani, S.G., Prasad, A.K., 2016. Experimental investigation of in-line and staggered blockages in parallel flowfield channels of PEM fuel cells. Int. J. Hydrogen Energy 41 (16), 6885–6893.

Holland, J.H., 1975. Adaptation in Natural and Artificial Systems: an Introductory Analysis with Applications to Biology, Control, and Artificial Intelligence. U Michigan Press.

Kang, K., Yoo, H., Han, D., Jo, A., Lee, J., Ju, H., 2016. Modeling and simulations of fuel cell systems for combined heat and power generation. Int. J. Hydrogen Energy 41 (19), 8286–8295.

Lemmon, E., Huber, M., McLinden, M., 2007. REFPROP, NIST Standard Reference Database 23, Version 8.0. National Institute of Standards and Technology, Gaithersburg, MD.

Li, X., Sabir, I., 2005. Review of bipolar plates in PEM fuel cells: flow-field designs. Int. J. Hydrogen Energy 30, 359–371.

Long, R., Li, B., Liu, Z., Liu, W., 2015. A hybrid system using a regenerative electrochemical cycle to harvest waste heat from the proton exchange membrane fuel

cell. Energy 93, 2079–2086.
Mann, R.F., Amphlett, J.C., Hooper, M.A.I., Jensen, H.M., Peppley, B.A., Roberge, P.R., 3//2000. Development and application of a generalised steady-state electrochemical model for a PEM fuel cell. J. Power Sources 86, 173–180.
Miansari, M., Sedighi, K., Amidpour, M., Alizadeh, E., Miansari, M., 2009. Experimental and thermodynamic approach on proton exchange membrane fuel cell performance. J. Power Sources 190, 356–361.
Murugesan, K., Senniappan, V., 2013. Investigation of water management dynamics on the performance of a Ballard-Mark-V proton exchange membrane fuel cell stack system. Int. J. Electrochem. Sci. 8, 7885–7904.
Nguyen, H.Q., Aris, A.M., Shabani, B., 2016. PEM fuel cell heat recovery for preheating inlet air in standalone solar-hydrogen systems for telecommunication applications: an exergy analysis. Int. J. Hydrogen Energy 41 (4), 2987–3003.
Omer, A.M., 2008. Energy, environment and sustainable development. Renew. Sustain. Energy Rev. 12, 2265–2300.
Peighambardoust, S.J., Rowshanzamir, S., Amjadi, M., 9//2010. Review of the proton exchange membranes for fuel cell applications. Int. J. Hydrogen Energy 35, 9349–9384.
Saeed, E.W., Warkozek, E.G., 2015. Modeling and analysis of renewable PEM fuel cell system. Energy Procedia 74, 87–101.
Sivanandam, S., Deepa, S., 2007. Introduction to Genetic Algorithms. Springer Science & Business Media.
Song, Y., Wang, J., Dai, Y., Zhou, E., 2012. Thermodynamic analysis of a transcritical CO 2 power cycle driven by solar energy with liquified natural gas as its heat sink. Appl. Energy 92, 194–203.
Van Nguyen, T., Knobbe, M.W., 2003. A liquid water management strategy for PEM fuel cell stacks. J. Power Sources 114, 70–79.
Vandani, A.M.K., Bidi, M., Ahmadi, F., 12//2015. Exergy analysis and evolutionary optimization of boiler blowdown heat recovery in steam power plants. Energy Convers. Manag. 106, 1–9.
Wang, C., Nehrir, M.H., Shaw, S.R., 2005. Dynamic models and model validation for PEM fuel cells using electrical circuits. Energy Convers. IEEE Trans. 20, 442–451.
Wang, J., Wang, J., Dai, Y., Zhao, P., 2014. Thermodynamic analysis and optimization of a transcritical CO_2 geothermal power generation system based on the cold energy utilization of LNG. Appl. Therm. Eng. 70, 531–540.
Wu, J., Yuan, X.Z., Martin, J.J., Wang, H., Zhang, J., Shen, J., et al., 2008. A review of PEM fuel cell durability: degradation mechanisms and mitigation strategies. J. Power Sources 184, 104–119.
Xia, G., Sun, Q., Cao, X., Wang, J., Yu, Y., Wang, L., 2014. Thermodynamic analysis and optimization of a solar-powered transcritical CO 2 (carbon dioxide) power cycle for reverse osmosis desalination based on the recovery of cryogenic energy of LNG (liquefied natural gas). Energy 66, 643–653.
Yang, P., Zhang, H., 2015. Parametric analysis of an irreversible proton exchange membrane fuel cell/absorption refrigerator hybrid system. Energy 85, 458–467.
Zhao, P., Wang, J., Gao, L., Dai, Y., 2012. Parametric analysis of a hybrid power system using organic Rankine cycle to recover waste heat from proton exchange membrane fuel cell. Int. J. Hydrogen Energy 37, 3382–3391.
Zhao, P., Wang, J., Dai, Y., Gao, L., 2015. Thermodynamic analysis of a hybrid energy system based on CAES system and CO 2 transcritical power cycle with LNG cold energy utilization. Appl. Therm. Eng. 91, 718–730.